The Astrophysical Journal, 684:364–372, 2008 September 1
© 2008. The American Astronomical Society. All rights reserved. Printed in U.S.A.

AN ACCURATE DISTANCE TO HIGH-VELOCITY CLOUD COMPLEX C

C. Thom,[1] J. E. G. Peek,[2] M. E. Putman,[3] Carl Heiles,[2] K. M. G. Peek,[2] and R. Wilhelm[4]
Received 2007 December 4; accepted 2008 May 6

ABSTRACT

We report an accurate distance of $d = 10 \pm 2.5$ kpc to the high-velocity cloud Complex C. Using high signal-to-noise ratio Keck HIRES spectra of two horizontal-branch stars, we have detected Ca II K absorption lines from the cloud. Significant nondetections toward a further three stars yield robust lower distance limits. The resulting H I mass of Complex C is $M_{\rm H\,I} = 4.9^{+2.9}_{-2.2} \times 10^6\ M_\odot$; a total mass of $M_{\rm tot} = 8.2^{+4.6}_{-2.6} \times 10^6\ M_\odot$ is implied, after corrections for helium and ionization. At 10 kpc, Complex C has physical dimensions 3×15 kpc, and if it is as thick as it is wide, then the average density is $\log\langle n\rangle \simeq -2.5$. We estimate the contribution of Complex C to the mass influx may be as high as $\sim 0.14\ M_\odot\ {\rm yr}^{-1}$.

Subject headings: Galaxy: evolution — Galaxy: halo — ISM: clouds — ISM: individual (Complex C)

Online material: color figure

1. INTRODUCTION

The halo of the Milky Way (MW) contains clouds of neutral hydrogen (H I) gas representing the flow of baryons into, and out of, the Galactic disk. Identified by their velocities, these high-velocity clouds (HVCs)[5] have been observed in H I 21 cm emission for more than 40 years (Muller et al. 1963). Since their distances cannot be determined by the application of a kinematic model, the mass scale of the flow is uncertain, and the clouds' origin and impact on the disk are open to speculation.

Since their discovery, many explanations have been offered for the HVC phenomenon, with a corresponding range of distances; most of these explanation can be traced to Oort (1966). One possible origin for some HVCs is a supernova-driven Galactic fountain, in which gas is expelled from the disk into the halo, condenses, and then returns in a cyclic flow (Bregman 1980; Houck & Bregman 1990). Gibson et al. (2001) suggested that this model may be appropriate for Complex C, based on observed abundance variations across the complex. In other galaxies, there is evidence that some (but not all) of the extraplanar H I observed in the edge-on spiral NGC 891 originates in such a fountain (Oosterloo et al. 2007). Theoretical models suggest that fountain gas may rise as high as $\sim$10 kpc above the disk (de Avillez 2000). Dwarf galaxy accretion is another avenue for mass input; the well-known Magellanic Stream (Mathewson et al. 1974; Putman et al. 2003) is the canonical example, but this mechanism has been suggested for other MW satellites (Putman et al. 2004). Another recent proposal posits the clouds to be condensing out of the hot MW halo (Maller & Bullock 2004; Kaufmann et al. 2006; Sommer-Larsen 2006; Peek et al. 2008), at a range of distances up to $\sim$150 kpc. Peek et al. (2008) suggested that HVC masses are inversely proportional to their distance, reasoning that condensing clouds are small at large distance, and form the seeds of the large HVC complexes, into which they grow via accretion as they approach the disk. If this scenario is correct, then all the large HVC complexes would be close ($d \sim 10$–15 kpc).

Complex C was first mapped by Hulsbosch & Raimond (1966). Its large angular size ($\sim$1600 deg^2) means that a number of UV-bright quasars align with high column density gas, allowing metallicity determinations by absorption-line spectroscopy. Based on a metallicity measurement of $\sim 0.1\ Z_\odot$, Wakker et al. (1999) suggested that Complex C is a low-metallicity, infalling cloud, fueling Galaxy formation. Gibson et al. (2001) later reported metallicities as high as 0.3 $Z_\odot$, proposing that Complex C may instead a be product of star formation in the Galaxy or a disrupted satellite. Most recently, Collins et al. (2007) confirmed this evidence of abundance variations across the cloud, independent of ionization effects, suggesting the possible mixing of primordial and enriched gas (see also Tripp et al. 2003).

There is no convincing evidence of dust in Complex C (e.g., Collins et al. 2003) nor any detections of molecular hydrogen (Murphy et al. 2000; Richter et al. 2001). Observations with the Wisconsin Hα Mapper (WHAM) have detected Hα emission at the same velocities as the H I emission (Tufte et al. 1998; Haffner et al. 2003). Higher ionization species, such as C IV, Si IV, N V, and O VI have been seen in absorption toward QSOs (Sembach et al. 2003; Fox et al. 2004). Fox et al. (2004) studied the O VI and other highly ionized species, concluding that they are most likely to arise in conductive or turbulent interface regions between the warm neutral gas seen in H I and the surrounding hot halo medium.

HVCs are often invoked by Galactic chemical evolution models as a source of infalling star formation fuel, which is needed in order to reproduce the metallicity distribution function of stars in the solar neighborhood (the G dwarf problem; e.g., Pagel & Patchett 1975; Alibés et al. 2001). As the largest HVC on the sky, Complex C could potentially contribute a significant fraction of the Galaxy's future star formation fuel. For H I clouds, the mass is related to the distance by $M_{\rm H\,I} = 0.236 S d^2$, where S is the total H I flux observed (in Jy km s^{-1}) and d is the distance in kpc. For Complex C, $S = 2 \times 10^5$ Jy km s^{-1} (Wakker & van Woerden 1991). Recently, Wakker et al. (2007) reported a firm distance limit to Complex C of 3.7–11.2 kpc, with a weaker limit of

[1] Department of Astronomy and Astrophysics, and Institute for Cosmological Physics, University of Chicago, Chicago IL, 60637; cthom@uchicago.edu.
[2] Astronomy Department, University of California, Berkeley CA, 94720; goldston@astro.berkeley.edu, heiles@astro.berkeley.edu, kpeek@astron.Berkeley.edu.
[3] Department of Astronomy, University of Michigan, Ann Arbor, MI 48109; mputman@umich.edu.
[4] Department of Physics, Texas Tech University, Lubbock, TX 79409; ron.wilhelm@ttu.edu.
[5] HVCs are defined as having $|v_{\rm LSR}| > 90$ km s^{-1} and hence do not corotate with the Galaxy.

TABLE 1
JOURNAL OF OBSERVATIONS

Target	l (deg)	b (deg)	g_0 (mag)	S/N	$v_{\rm helio}$ (km s^{-1})	Distance (kpc)	Label
SDSS J173424.01+601735.3	89.1	32.8	15.9	60	−482.6 ± 1.4	12.8 ± 3.2	S135
SDSS J172009.78+612502.3	90.6	34.4	14.7	100	−322.3 ± 3.3	7.8 ± 2.0	S139
SDSS J150335.53+623513.5	100.7	48.4	15.6	60	−201.2 ± 2.5	11.3 ± 2.8	S437
SDSS J153915.24+575731.7	91.2	47.5	15.9	80	−14.4 ± 1.5	10.2 ± 2.6	S441
SDSS J133654.82+622241.5	114.0	54.0	15.4	65	26.5 ± 0.9	10.4 ± 2.6	S674

NOTE.—SDSS names are created from the right ascension and declination (J2000.0) of the object, truncating coordinates. Galactic coordinates have been rounded to 0.1°. Magnitudes are extinction-corrected g band, taken from the SDSS database. Signal-to-noise measures are given for the continuum region near Ca II K. For convenience, we label each star with a number, corresponding to its numerical position in the catalog of Sirko et al. (2004).

6.7–11.2 kpc. Here we employ high-quality Keck spectra to determine the most accurate measurement of d for Complex C to date.

2. DATA

Five horizontal-branch stars from the catalog of Sirko et al. (2004) that align with Complex C were observed with the High Resolution Echelle Spectrometer (HIRES; Vogt et al. 1994) on the Keck I telescope on 2007 June 8 and June 9 (UT). We employed the UV cross-disperser to maximize throughput at Ca II K (3933.663 Å) and binned the data 2× in the spatial direction. In this configuration, the Na I D lines are within our wavelength coverage, but are at the extreme edge of the order. The $7'' \times 0.8''$ slit yielded a resolution of $R \sim 48,000$. Over the course of the two nights, the seeing varied from ∼1.2″ to 1.8″, but we nevertheless obtained excellent quality data. Table 1 summarizes our targets. For these stars, stellar parameters were obtained using the techniques described in Wilhelm et al. (1999). Absolute magnitudes and distances for the stars were determined by comparing $T_{\rm eff}$, log g, and [Fe/H] to the run of theoretical isochrones of Girardi et al. (2004) and Dorman (1992); distances are given in the text and in Table 4. External tests of the stellar technique against stars in globular clusters indicate that distances are accurate to ∼25% (R. Wilhelm et al. 2008, in preparation). We thus adopt a 25% error as our formal distance error; in all cases, this error is greater than that estimated from the stellar classification, sometimes significantly. Continuing calibration efforts of the Segue Stellar Parameter Pipeline (Lee et al. 2008) should improve this accuracy in the future.

To reduce the data, we used the HIRES Redux pipeline (R. Bernstein et al. 2008, in preparation), which is distributed as part of the `xidl` package.[6] The package applies standard bias and flat-field corrections, performs a two-dimensional wavelength calibration, and extracts the individual orders to give final one-dimensional spectra and associated errors. For equivalent width measurements, we fit the local continuum with a low-order Legendre polynomial and directly integrate the data, determining error contributions from both the noise and continuum fitting (Sembach & Savage 1992). In general, the HVC Ca II H (3968.467 Å) line is in the wings (and in some cases in the core) of the broad stellar Hϵ (3970.072 Å) line. The Hϵ line is sufficiently broad that it completely dominates the echelle order, and the true continuum cannot accurately be determined. Since we care only about the HVC Ca II H line, we fit a pseudocontinuum along the Balmer line wing, where possible, removing its contribution to the absorption.

[6] See http://www.ucolick.org/xavier/IDL/index.html.

H I spectra were primarily drawn from the combined Leiden/Argentine/Bonn (LAB) survey, which has a beamwidth of ∼36′(FWHM; Kalberla et al. 2005). In one case (S441; see Table 1), an H I spectrum from Effelsberg (9′ beam) is available. Heliocentric radial velocities (RVs) for all five stars were determined by fitting the positions of unblended metal lines in the echelle data. These are also given in Table 1. In most cases ∼30 or more lines were available, but for S139, only 12 unblended metal lines are available in our Keck spectrum. Errors on RVs are the 1 σ Gaussian dispersion of the ensemble of measured lines.

Using the absorption-line technique, upper or lower distance limits are placed on the distance to the HVC gas, based on the detection or nondetections of absorption lines due to the gas in the spectrum of stars at known distance. The technique is described in detail elsewhere (Schwarz et al. 1995; Thom 2006); Figure 1 of Schwarz et al. (1995) is particularly enlightening. Since the stars must lie at known (or knowable) distances, horizontal-branch and RR Lyrae stars are the most commonly used, but in principle, any hot star at known distance may be used; hot stars are desirable, to reduce the number of metal lines in the stellar spectrum, which may confuse the HVC absorption. In order to maximize the probability of optical detection, strong resonance transitions are the most appropriate. In the optical, Ca II H and K are the most common, but the Na I D lines may also be used (see, e.g., Thom et al. 2006). Strong UV transitions such as O I have also been used (Danly et al. 1993), and with the scheduled installation of the Cosmic Origins Spectrograph on the upcoming *Hubble Space Telescope* (*HST*) servicing mission, Mg II may also prove useful.

3. RESULTS

In the following subsections, we discuss the individual lines of sight, first for the detections, then for the nondetections. We consider the upper distance limits that are set by the detections, and the lower distance limits that can be set by the nondetections. Finally, we summarize our results, both in tabular and pictorial form.

3.1. *Detections*

S437, $d \sim 11$ kpc.—Toward the star S437 two HVC emission components can be seen in the H I spectrum available from the LAB survey (Fig. 1), at $v_{\rm LSR} = -115$ km s^{-1} and -165 km s^{-1}, with corresponding column densities N(H I) = 2.1 ± 0.3 and $(1.5 \pm 0.4) \times 10^{19}$ cm^{-2}. The HVC emission component at -115 km s^{-1} is clearly evident in absorption at Ca II K, but the corresponding Ca II H line is lost in the core of the Hϵ Balmer line. Since the HVC feature falls in the very core of the Hϵ line, we do not attempt to fit the continuum to the Balmer line wings. The HVC component at -165 km s^{-1} is lost in the strong stellar Ca II lines. Emission and absorption at $v_{\rm LSR} = -56$ km s^{-1} from

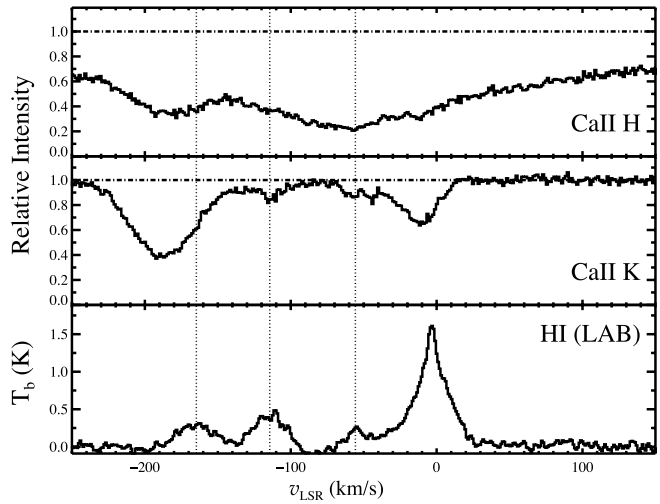

FIG. 1.—S437. Detection of Complex C in absorption toward S437. In this direction, we see the HVC in emission at $v_{LSR} = -115$ km s^{-1}, which is clearly seen in Ca II K absorption. There is also a higher velocity component seen in emission (sometimes called the "high-velocity ridge") at $v_{LSR} = -165$ km s^{-1}. This higher velocity component is not detected, since HVC Ca II K absorption is obscured by the stellar Ca II K line, and the Ca II H line is obscured by both the core of the stellar Hϵ line and the stellar Ca II H absorption. IVC gas is evident at $v_{LSR} = -56$ km s^{-1}.

the intermediate-velocity cloud (IVC) known as the "IV arch" can also be seen. This cloud is known to be nearby (0.4 kpc $< z <$ 3.5 kpc; Ryans et al. 1997).

S674, $d \sim 10$ kpc.—The optical spectra of S674, shown in Figure 2, provides a second detection toward the high-latitude part of Complex C. Absorption is detected from Complex C at $v_{LSR} = -127$ km s^{-1}, setting an upper distance limit. We also detect the nearby IV arch at $v_{LSR} = -48$ km s^{-1} and the MW disk in absorption. Note that we have fitted the Ca II H continuum along the wing of the stellar Hϵ Balmer line, removing it from Figure 2. The falloff in the continuum redward of $v_{LSR} =$ 100 km s^{-1} in the Ca II H line is where the Balmer line transitions from wing to core; since we use only a low-order polynomial and do not attempt to match the entire Balmer line profile, the fit breaks down in this region.

We clearly detect multiple absorption components in the optical spectra that do not always align well with the H I emission

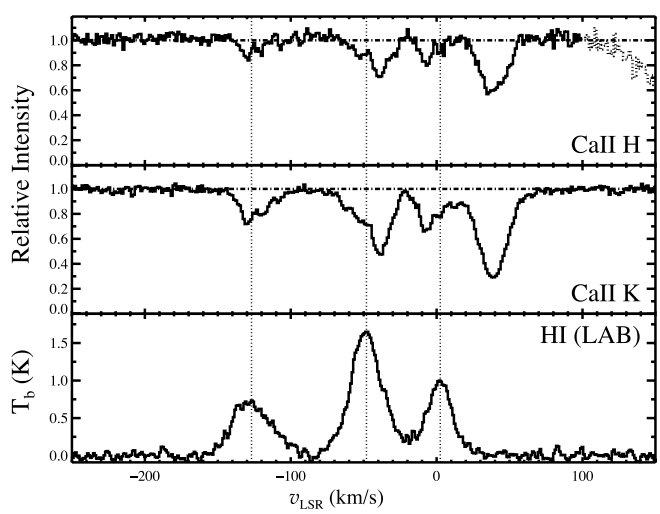

FIG. 2.—S674. Strong absorption from Complex C is evident at -127 km s^{-1}, setting an upper distance limit. Intermediate-velocity absorption from the IV arch can also be seen at -48 km s^{-1}. See text for further details.

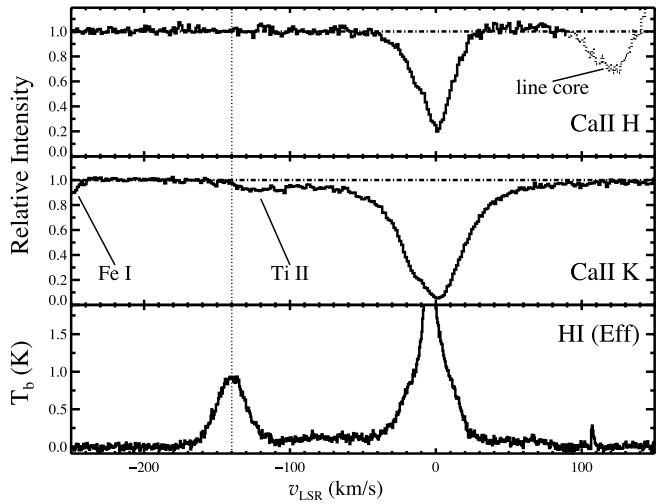

FIG. 3.—S441. No HVC absorption is present in the sight line toward S441. The weak feature in Ca II K redward of the HVC position is stellar Ti II. For the Ca II H profile, we fit a pseudocontinuum along the broad wing of the Hϵ Balmer line. The dotted section in this top panel marks the core of the Balmer line, where the continuum fit is unreliable.

positions. This is present in both the HVC absorption, as well as the IVC and disk gas. Since the H I data sample 36′ on the sky, while the optical data trace a pencil beam, this may be a consequence of beam smearing. An interferometer map would be required to confirm this. Note, however, that in all cases, the optical absorption falls within the line limits defined by the H I data.

3.2. *Nondetections*

S441, $d \sim 10$ kpc.—At roughly the same latitude as our two detections and only ~28′ from the Mrk 290 sight line, this line of sight has the most complicated optical spectrum. Figure 3 shows both the optical and radio spectra. Note that for this sight line, the H I spectrum comes from the Effelsberg telescope, which has a substantially smaller beam than the coarse resolution of the LAB survey.

The optical data in the Ca II K region show an absorption line slightly to the red ($v_{LSR} = -125$ km s^{-1}) of where we expect the HVC absorption to lie ($v_{LSR} = -140$ km s^{-1}). This line is *not* HVC absorption, but rather a Ti II line at a rest wavelength of 3932.020 Å (Meggers et al. 1976). This identification is made based on several factors. First, in the stellar rest frame, a fit to this line gives a rest wavelength 3932.00 Å. This differs from the expected position by only 1.6 km s^{-1}, in good agreement with the measured radial velocity precision (1.4 km s^{-1}). Second, the strength of this line is consistent with other Ti II lines in the spectrum of S441 with similar ionization potential and log gf. Finally, the strength of this line is $W_\lambda = 25.9 \pm 1.4$ mÅ. If this was an HVC Ca II K absorption line that was offset from the H I position, the corresponding Ca II H line would be 13 mÅ. The noise level in the Ca II H region [$\sigma(W_\lambda) = 2.5$ mÅ] is low enough that we would detect any HVC absorption at the 5 σ confidence level. We can thus exclude this possibility.

Since the stellar Ti II line only impinges on the wing of the expected HVC Ca II K absorption and is very well fit by a single Gaussian component, it does not diminish our ability to detect any putative HVC absorption line. Figure 4 shows the result of this fit. We include the strong stellar Ca II K line and a very weak unidentified line at rest wavelength 3932.25 Å ($v_{LSR} = -106$ km s^{-1}). Both these latter features are well outside the region of interest for HVC absorption. The lower panel shows the residual of the

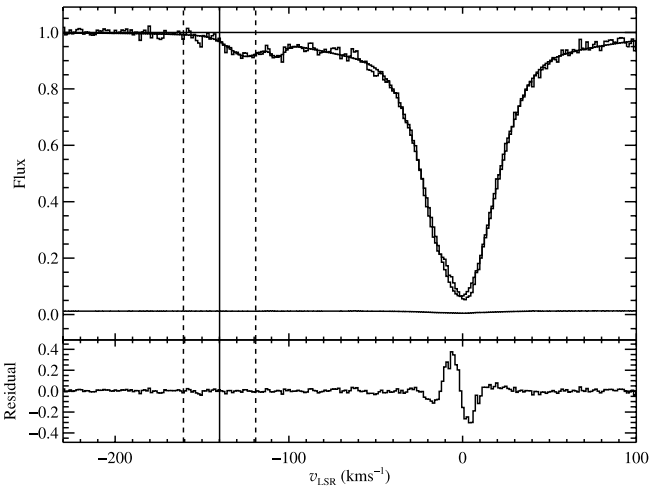

FIG. 4.—Fit to the stellar absorption in S441. The solid vertical line marks the expected HVC position. Dotted lines show the $\pm 2\ \sigma$ velocity range derived from the H I spectrum. See text for details. [*See the electronic edition of the Journal for a color version of this figure.*]

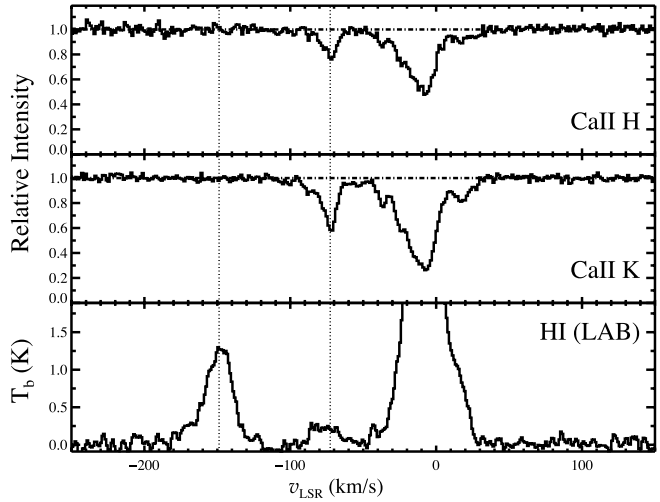

FIG. 5.—S135. No HVC absorption is evident at the expected velocity $v_{LSR} = -150$ km s^{-1}. Multicomponent IVC absorption can clearly be seen in both Ca II H and K absorption and H I emission. The strongest absorption component is at $v_{LSR} = -77$ km s^{-1}. Galactic absorption components, seen in both Ca II K and Ca II H, are visible in the range -40 km s$^{-1} \lesssim v_{LSR} \lesssim 20$ km s^{-1}, corresponding to the strong H I emission.

fit. The expected HVC position is marked by the solid line, while the dotted lines mark the $\pm 2\ \sigma$ line width limits (where σ is the Gaussian width of the H I spectrum). We emphasize that only the high quality of our Keck data allows us to cleanly remove the stellar absorption from the wing of the putative HVC region and place a significant lower distance limit on the cloud.

Since the S441 sight line is very close to the Mrk 290 sight line, this significantly strengthens the conclusions that can be drawn from the nondetection of both Ca II K and Ca II H, since we can be confident of the level of HVC absorption expected. The worst-case expected HVC absorption toward this line of sight is 38 mÅ (Ca II K) and 19 mÅ (Ca II H); both these would be clearly visible. Section 3.4 contains further discussion on the interpretation of nondetections.

S135, $d \sim 13$ kpc.—The two stellar probes S135 and S139 are both a few degrees from the edge of Complex C (See Fig. 7), at lower latitude than our earlier targets. For S135, our most distant target, we see no indication of HVC absorption, as shown in Figure 5. Unrelated IVC gas can clearly be seen in both H I emission and absorption at $v_{LSR} = -77$ km s^{-1} in both Ca II H and K. This IVC gas can be seen in the LAB data cube to connect smoothly with the Galactic plane at lower latitudes. Although it is not shown in Figure 5, we also see this IVC in the Na I D_2 line, which is the stronger of the two Na I D doublet lines. The lack of HVC absorption sets a lower distance limit of 12.8 ± 3.2 kpc.

S139, $d \sim 8$ kpc.—The optical spectra of S139 are our highest signal-to-noise data. Figure 6 shows that there is clearly no absorption detected corresponding to the strong HVC emission. The Ca II H position is at the very core of the Hϵ Balmer line, but the Ca II K data set a firm lower distance limit if 7.8 ± 2.0 km s^{-1}. The Galactic emission shows a broad emission wing to $v_{LSR} \sim -50$ km s^{-1}; Ca II K absorption components are also seen in this range. There is some evidence of IVC emission, with corresponding very weak absorption, in the range $v_{LSR} = 70$–100 km s^{-1}, but better data are needed to confirm this. The lack of HVC absorption sets a lower distance limit.

3.3. *Upper Distance Limits*

Table 2 gives the results of the two detections of Complex C in absorption toward background stars. In this table, column (1) lists our target name. Stellar distances and measured H I column densities are given in columns (2) and (3), respectively. Column (4) gives the measured Ca II K equivalent width and its 1 σ error. Column (5) lists the corresponding column density for this equivalent width, N(Ca II), assuming the gas is optically thin. Columns (3) and (5) are combined to give the ratio N(Ca II)/N(H I), which is sometimes called the "abundance" and denoted A(Ca II). This is given in column (6). Both sight lines have the same Ca II abundance to within errors and are also in good agreement with the values observed toward the QSO sight lines Mrk 290 and PG 1351+640, up to 20° away (see below). Such good agreement suggests that there are not large variations of the Ca II abundance across the cloud.

3.4. *Lower Distance Limits*

Nondetections are harder to interpret than detections; one must be convinced that the lack of absorption is not a random confluence of bad luck. In general, one predicts the strength of the absorption that should be seen if the star is behind the gas by using the measured N(Ca II)/N(H I) ratio in the cloud and the H I

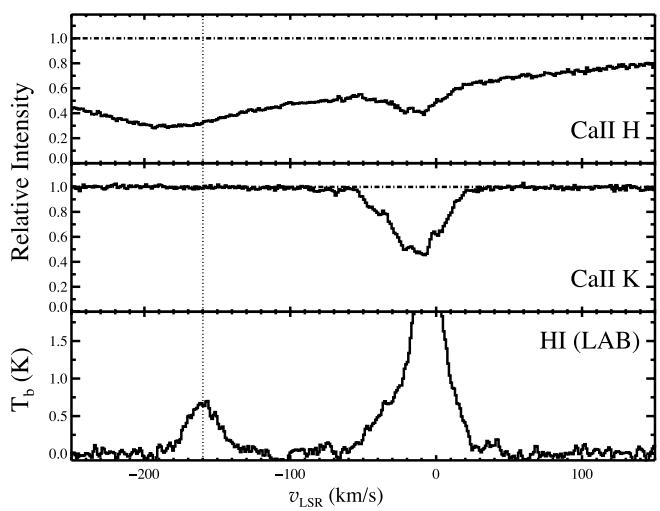

FIG. 6.—S139. No Ca II K absorption can be seen corresponding to the HVC emission at $v_{LSR} = -160$ km s^{-1}. The Ca II H line falls in the core of the stellar Hϵ line.

TABLE 2
Summary of Upper Limits

Target (1)	Distance (kpc) (2)	N(H I) ($\times 10^{19}$cm^{-2}) (3)	$W_\lambda \pm \sigma(W_\lambda)$ (mÅ) (4)	N(Ca II) ($\times 10^{19}$cm^{-2}) (5)	A(Ca II) (6)
S437	11.3 ± 2.8	2.1 ± 0.3	46.9 ± 2.0	5.5 ± 0.2	$(26 \pm 4) \times 10^{-9}$
S674	10.4 ± 2.6	4.0 ± 0.5	76.5 ± 1.8	8.9 ± 0.2	$(22 \pm 3) \times 10^{-9}$

Notes.—Summary of measurements for upper limits. N(H I) is taken from the LAB survey for both stars. The measured equivalent widths are for the Ca II K HVC line. Column densities assume a linear curve of growth. The final column gives the Ca II to H I column density ratio, which is referred to as "abundance," A(Ca II), and is measured in parts per billion.

column density toward the star to infer N(Ca II). This, in turn, provides the expected equivalent width of the Ca II absorption line. We then attempt to show that the data are of sufficient quality as to clearly detect absorption lines of that strength.

Wakker (2001) has argued that one should adopt a worst-case scenario to interpret nondetections; in this view—which we adopt here—it is not sufficient that the expected absorption be significantly stronger than the detection level, but we must account for the case in which every factor works against a detection. For example, the gas-phase abundance may be lower than expected, the column density may be lower than expected, and so on. This is quantified in the notion of multiplicative "safety factors," which are given for a range of effects. The predicted absorption strength is reduced by all these safety factors to obtain a worst-case absorption strength; only cases in which the noise level is less than this worst case are deemed "strong" or significant nondetections. We refer the interested reader to the Appendix of Wakker (2001) for a more complete discussion of all these effects.

The comparison of large-beam 21 cm measurements of N(H I) to pencil-beam optical or UV data is difficult, because unresolved small-scale structure can potentially introduce systematic errors. Our H I column densities are mostly taken from the LAB survey, which samples 36′ of sky, or in one case, Effelsberg (9′). Both of these sources have significantly larger beams than the pencil beam of the optical data. This may be clearly seen, for example, in the spectra of S674 (Fig. 2), where the optical data show clear multicomponent absorption structure, yet the H I emission spectrum does not. Systematic uncertainties are therefore likely to be present, since the radio and optical spectra sample different areas on the sky.

No comprehensive study exists comparing N(H I) measured at a range of spatial scales toward a large number of sight lines. The best study is that of Wakker et al. (2001), who compared measurements at 36′, at 9′, and pencil-beam UV Lyα measurements on six QSO and two stellar sight lines (only two toward Complex C). They concluded that most measurements at 9′ are accurate to within about 25%, while the larger 36′ beam gives an uncertainty of up to a factor of 3. This is in line with the results of Savage et al. (2000), who compared 10 UV Lyα measurements of N(H I) to those of the 21′ beam of the NRAO 43 m dish, finding that $N(\text{H I})_{\text{Ly}\alpha}/N(\text{H I})_{21\,\text{cm}}$ ranges between 0.62 and 0.91. Thus, we adopt a safety factor of 2× for the S441, where 9′ Effelsberg data are available. For the other sight lines, a safety factor of 3× is warranted. We caution that variations may be still greater in cloud cores (Wakker et al. 2002) and also note that both the above cited works have only 8–10 Lyα measurements of N(H I). Clearly, this is the most uncertain aspect of our results, and we are pursuing interferometer data (e.g., with the Allen Telescope Array [ATA]) for our sight lines.

Complex C shows little evidence of dust depletion (Collins et al. 2003), so we do not take into account depletion effects. In the ideal case, the gas-phase abundance toward the stellar sight line will be known from measurements of nearby extragalactic sight lines. This is the case for S441, which is very close (<0.5°) to the Mrk 290 sight line. For the S135 and S139 sight lines, however, we must take into account possible variations in gas metallicity and ionization conditions. Since Ca II is not the dominant ionization stage of Ca in the interstellar medium (ISM) and HVCs, a safety factor of 2× is included to account for this (Wakker 2001). Several authors have shown evidence that the metallicity of Complex C varies from one QSO sight line to another in the range 0.1–0.3 $Z_\odot$, independent of ionization effects (e.g., Gibson et al. 2001; Collins et al. 2007). This may be a result of Complex C mixing with local enriched gas (Gibson et al. 2001; Tripp et al. 2003). Ca II abundances have been measured toward only two sight lines: Mrk 290 [A(Ca II) $= 21 \times 10^{-9}$] and PG 1351+640 [A(Ca II) $= 18 \times 10^{-9}$] (Wakker et al. 1996; Wakker 2001). Mrk 290 is closest to the S135 and S139 sight lines, so we adopt the measured abundance and include a safety factor of 3×, in line with the metallicity variations.

Table 3 provides a summary of the process used to determine the significance of the nondetections. Column (1) provides target name. Column (2) gives the stellar distance. The measured N(H I) toward the star is listed in column (3). Column (4) shows the predicted absorption equivalent width, $W_{\lambda,\text{pred}}$. To calculate this value, we assume that the gas is optically thin and adopt A(Ca II) $= 21 \times 10^{-9}$. Column (5) lists the safety factor adopted, with column (6) giving the resulting strength of any putative absorption line, reduced by this safety factor. Column (7) lists the 1 σ equivalent width error, integrating over a line width determined from the H I data. Finally, column (8) gives the significance of the nondetection. Following Wakker (2001), a significance greater than 1 is considered a "strong" lower distance limit, with values lower than 1 providing "weak" limits.

Table 3 shows that even under pessimistic assumptions, the excellent quality of the Keck data gives us confidence in our nondetections. For the sight line toward S441, the safety factor according to the above prescription is significantly smaller than the other two sight lines, since the H I column density is more accurately known, and the Ca^+ abundance of the gas in this region is well measured. Nevertheless, a factor of 2× is almost certainly too optimistic. In line with this concern, we include in Table 3 a second assessment of the significance of this nondetection, using the same 18× factor as for S135 and S139. Even in this scenario, any putative HVC absorption would still be detected. We conclude that all our nondetections provide strong lower distance limits to Complex C.

3.5. *Summary of Results*

We summarize our results in Table 4. This table gives the Galactic coordinates and stellar distances for each target and indicates whether the target provides an upper (U) or lower (L)

TABLE 3
SUMMARY OF LOWER LIMITS

Target (1)	Distance (kpc) (2)	N(H I) ($\times 10^{19}$cm^{-2}) (3)	$W_{\lambda,\mathrm{pred}}$ (mÅ) (4)	Safety Factor (5)	$W_{\lambda,\mathrm{saf}}$ (mÅ) (6)	$\sigma(W_\lambda)$ (mÅ) (7)	Significance (8)
S135	12.8 ± 3.2	4.9 ± 0.4	88.8	18	4.9	±1.6	3.1
S139	7.8 ± 2.0	3.3 ± 0.4	60.2	18	3.3	±1.1	3.0
S441	10.2 ± 2.6	4.2 ± 0.2	75.3	2	37.7	±1.7	22.2
S441	10.2 ± 2.6	4.2 ± 0.2	75.3	18	4.2	±1.7	2.5

NOTES.—Summary of measurements for lower limits. The source of distances and N(H I) is described in the text. We give the predicted Ca II K equivalent width before and after taking into account the safety factors, as well as the safety factor adopted for each target. The contributions to these numbers are discussed in § 3.4. The significance of the nondetections is given as the ratio $W_{\lambda,\mathrm{saf}}/\sigma(W_\lambda)$. The final column tabulates the abundance N(Ca II)/N(H I) used to derived the predicted equivalent widths, also discussed in § 3.4.

distance limit to Complex C. Figure 7 shows an H I column density map of Complex C in Galactic coordinates, using an orthogonal projection. Contours are drawn at log N(H I) = 18.2, 19.0, 19.7. The stellar lines of sight are marked with star symbols in the case of detections and crosses in the case of nondetections. The stars are labeled, along with the corresponding stellar distances. We also mark the position of the Mrk 290 and PG 1351+640 sight lines (hourglasses), along which the Ca II abundance is measured.

For orientation, we also show Complex C in perspective view in Figure 8. This figure shows the position of the gas in relation to the Galactic center and the solar position. Filled circles in this diagram show the HVC detections, S437 and 674. Open circles show the positions of the nondetections, S135, S139, and S441. For all stars, we also show their position projected onto the plane of the Galaxy. The 1 σ distance error bars are indicated for each star. The shape and orientation of Complex C in this diagram should be taken as indicative only.[7] An accurate representation would require more distance constraints, especially in the low-latitude, low-longitude regions (rightmost part in this representation).

Taken together, our distance limits imply a canonical distance of 10 ± 2.5 kpc to Complex C in the higher latitude regions. Toward S674 at the highest longitudes, the HVC is constrained to be closer than 10.4 ± 2.6 kpc. In the middle latitudes, both the upper limit from S437 ($d < 11.3 \pm 2.8$ kpc) and lower limit set by S441 ($d > 10.2 \pm 2.6$ kpc) are consistent with the 10 kpc distance. At lower latitudes, we have only lower limits from S135 ($d > 12.8 \pm 3.2$ kpc) and S139 ($d > 7.8 \pm 2.0$ kpc). While both these stars are consistent with a 10 kpc distance for Complex C, we have no limits for the low-latitude parts of the complex and cannot exclude the possibility of a distance gradient. It would not be surprising if the lower latitude, lower longitude parts of the complex were more distant, given the large angular size of Complex C. Observations at high latitudes of closer stars in the range 6–8 kpc and of more distant stars in the lower longitude, lower latitude regions are needed to substantiate this speculation. We stress that the ~25% distance accuracy is the current limit of stellar classification techniques for horizontal-branch stars and applies to *all* results; a systematic calibration effort is required to reduce this uncertainty.

[7] Indeed, recent H I data show Complex C extends much closer to the plane, although it is no longer a single coherent structure at these latitudes.

TABLE 4
SUMMARY OF DISTANCE LIMITS

Target	l (deg)	b (deg)	Distance (kpc)	Type
S135	89.1	32.8	12.8 ± 3.2	L
S139	90.6	34.4	7.8 ± 2.0	L
S437	100.7	48.4	11.3 ± 2.8	U
S441	91.2	47.5	10.2 ± 2.6	L
S674	114.0	54.0	10.4 ± 2.6	U

NOTES.—Summary of our distance limits. Coordinates are Galactic and are provided to the nearest 1/10th of a degree. The distance to each star is listed, with an indication whether the star provides a lower (L) or upper (U) distance limit.

4. DISCUSSION

For ease of discussion, we first consider Complex C to be at a uniform distance of 10 kpc. With such a large projected size, this is unlikely unless Complex C has a curved geometry. Using the total flux for Complex C (Wakker & van Woerden 1991), our distance limit implies a mass for Complex C of $M = 4.9^{+2.8}_{-2.2} \times 10^6\ M_\odot$. To calculate the total mass, we include a factor of 1.4 to account for helium and an ionization fraction $M_{\mathrm{H}^+} = 0.18 M_{\mathrm{H\,I}}$ (Wakker et al. 1999; Sembach et al. 2003). Since there is no indication of molecular gas (Murphy et al. 2000; Richter et al. 2001), we take $M_{\mathrm{H}} = M_{\mathrm{H}^+} + M_{\mathrm{H\,I}}$ H I and derive a total mass for Complex C of $M_{\mathrm{tot}} = 8.2^{+4.6}_{-2.6} \times 10^6\ M_\odot$.

For comparison, Complex C has an H I mass of order the mass that Lockman (2003) derived for Complex H by assuming that it is a satellite of the MW merging with the outer disk. Of the low-luminosity dwarf galaxies recently discovered in the Sloan Digital Sky Survey (SDSS; e.g., Willman et al. 2005a, 2005b; Belokurov et al. 2006, 2007), only Leo T has been shown to have associated neutral gas (Ryan-Weber et al. 2008); the H I mass of Complex C is more than an order of magnitude more than that of Leo T and is comparable to other local group dwarf irregulars, such as Pegasus, DDO 210, and LGS 3 (Mateo 1998). Complex C is also an order of magnitude more massive than the HVCs surrounding the M31/M33 system (Westmeier et al. 2005). Despite the large masses of neutral gas, a variety of searches have failed to find any evidence for an associated stellar content with any HVC (e.g., Willman et al. 2002; Simon & Blitz 2002; Siegel et al. 2005; Simon et al. 2006), and there is no evidence of a connection between Complex C and any dwarf galaxies.

The calculation of the mass flux onto the Galaxy that Complex C provides is hampered by our ignorance of the tangential velocity, which limits our ability to determine the vertical velocity with respect to the disk. We attempt to average over much of our ignorance by considering the average mass flow over the whole accretion timescale (i.e., the time it takes for the whole complex to accrete). The farthest gas from the plane, at highest latitudes, is that between $b = 55°$ and 60°. We choose a representative direction $(l, b) = (120°, 58°)$. At $d = 10$ kpc, this gas is ~8 kpc above the disk and has a line-of-sight velocity $v_{\mathrm{LSR}} = -126$ km s^{-1}. To

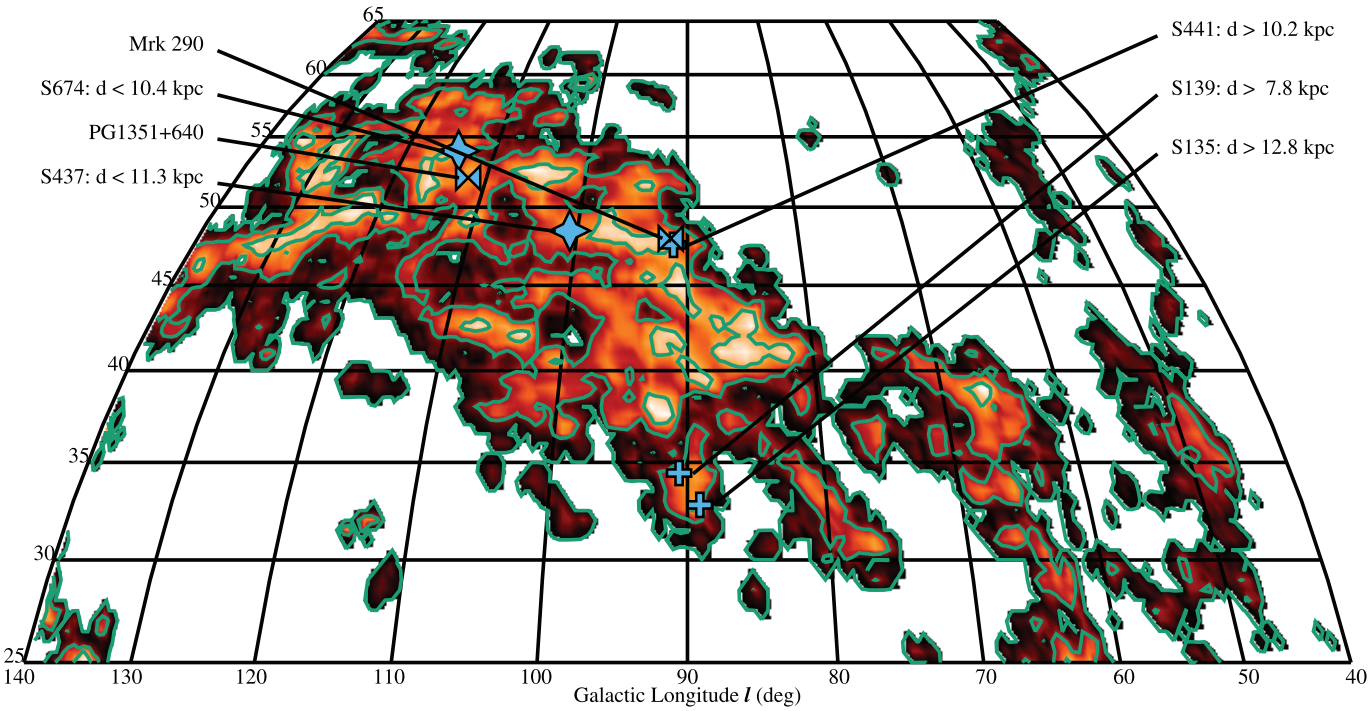

FIG. 7.—Location of SDSS stellar targets with respect to H I emission of Complex C. Contours are drawn at $\log N(\mathrm{H\ I}) = 18.2$, 19.0, and 19.7.

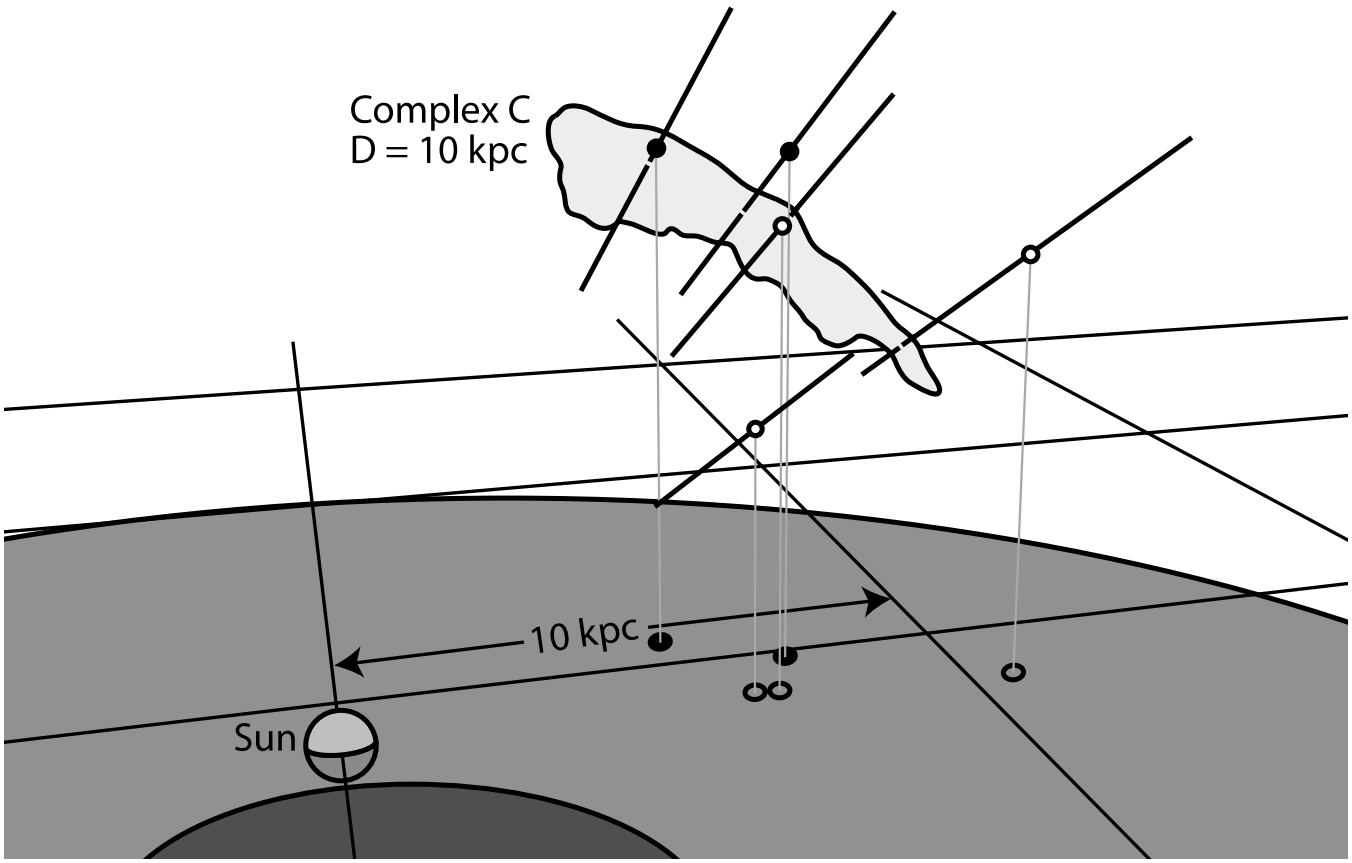

FIG. 8.—Diagram showing the position of Complex C in relation to the Sun. The inner Galaxy is indicated by the dark region at the bottom. HVC detections are marked by full circles, nondetections by open circles. The positions of stellar targets projected onto the Galactic plane and 1 σ distance error bars are also shown. Note that the shape of Complex C here is *not* an accurate depiction and is indicative only.

remove the disk rotation, we convert to deviation velocity, which is the amount by which the gas deviates from a model of Galactic rotation (de Heij et al. 2002), giving $v_{\rm dev} = -105$ km s^{-1}. We consider three cases. First, we assume that the tangential component of the velocity is equal to the radial component and consider both extremes, in which this tangential component is directed toward and away from the disk. This results in a range of vertical velocities $v_z = -34$ to -145 km s^{-1}, where the negative indicates a direction toward the disk. The case in which the motion is purely radial (i.e., no tangential component) is intermediate to these two extremes, having simply $v_z = -105 \sin 58^\circ = -89$ km s^{-1}. This range of velocities results in a range of accretion timescales 60–250 Myr and a corresponding mass flux in the range 0.03–0.14 $M_\odot$ yr^{-1}. It is worth noting that Tripp et al. (2003) have argued that the lower latitude parts of Complex C show signs of interaction with the thick disk or lower halo.

The condensing-cloud model (Sommer-Larsen 2006; Peek et al. 2008) predicts $\sim$0.2 $M_\odot$ yr^{-1} of accretion coming from HVCs. Meanwhile, chemical evolution models require such infall to reproduce the observed metallicity distribution in the disk (Alibés et al. 2001; Fenner & Gibson 2003). The most recent calculations suggest an infall rate of $\sim$1 $M_\odot$ yr^{-1} about 5 Gyr ago, falling roughly to half that at the present epoch (Chiappini et al. 2001). Thus, Complex C may provide a substantial amount of the required mass flux on the Galaxy, although the question of how this H I is converted into stars remains.

Now that we have established the distance to Complex C, we can also attempt to put some constraints on physical parameters such as length scales and density. Clearly, the density will vary from sight line to sight line for a large, inhomogeneous structure like Complex C, and the numbers we derive here should be taken as indicative only. For a canonical distance $d = 10$ kpc, simple geometry implies a transverse scale factor $\sim$0.175 kpc deg^{-1}. If we take two representative points on the extreme edges of the cloud, $(l, b) = (90, 50)$ and (110,40), the maximum angular extent across Complex C is $\theta \approx 17^\circ$, which corresponds to a physical distance $L \approx 3.0$ kpc. To assess the length of Complex C, we take the points[8] $(l, b) = (30, 15)$ and (130, 55), which correspond to a length $\sim$15 kpc. Lower latitude and longitude gas is present, but its direct connection with Complex C is ambiguous, since it blends with disk emission. By comparison, the Magellanic Stream is approximately 10 kpc $\times$ 100 kpc in size, with a mass of $\sim 2 \times 10^8$ $M_\odot$, for an assumed distance of 55 kpc (Putman et al. 2003). If we further assume that the complex is as deep as it is wide, then the average density, $\langle n \rangle$, along the line of sight may be computed. Toward the two stars that provide upper limits, S437 and S674, we then have $\log n = -2.6$ and -2.4, respectively.

5. CONCLUSION

We have used the presence and absence of Ca II K absorption in five stars aligned with the high-velocity cloud Complex C to derive a distance to the complex of 10 $\pm$ 2.5 kpc. At high latitude, we detect HVC gas in absorption toward stars $\sim$10 and $\sim$11 kpc away, setting upper distance limits. At similar latitudes, a nondetection provides a lower limit of $\sim$10 kpc. Nondetections in stars at $\sim$8 and $\sim$13 kpc at lower latitudes are consistent with this distance. Since the stellar distances are accurate to $\sim$25%, a canonical distance of 10 $\pm$ 2.5 kpc is set, but we cannot exclude the possibility of a distance gradient, which would mean larger distances for lower latitude parts of Complex C. Indeed, such a distance gradient would be expected when one considers the large angular size of the complex.

The distance implies an H I mass for Complex C of $M_{\rm H\,I} = 4.9^{+2.8}_{-2.2} \times 10^6$. Applying corrections for helium and ionized gas yields total mass of Complex C $M_{\rm tot} = 8.2^{+4.6}_{-2.6} \times 10^6$ $M_\odot$. We derive a mass inflow rate in the range 0.03–0.14 $M_\odot$ yr^{-1}, with the uncertainty mostly coming from the unknown tangential velocity of Complex C. If there is no tangential velocity component, this inflow rate is $\sim$0.1 $M_\odot$ yr^{-1}. Thus, Complex C may provide a significant fraction of the infall rate predicted by the condensing-cloud model. At the measured distance, Complex C is some $\sim$3 kpc across, with an average density of order $\log n = -2.5$. Our accurate distance contributes to a picture in which the large HVC complexes are nearby Galactic objects, with many of them now known to be within $d < 10$–15 kpc (van Woerden et al. 1999; Thom et al. 2006; Wakker et al. 2007, 2008). The question of whether the compact HVCs are part of this same population remains open, although condensation models place these small, isolated clouds at larger distances. With the first elements to a solution to the high-velocity cloud distance problem now well established, continuing efforts will provide a more complete census of neutral gas in the Milky Way halo.

We thank Tobias Westmeier for providing the HVC data from which Figure 7 was made and for the Effelsberg spectrum toward S441. The optical data presented herein were obtained at the W. M. Keck Observatory, which is operated as a scientific partnership among the California Institute of Technology, the University of California, and the National Aeronautics and Space Administration. The Observatory was made possible by the generous financial support of the W. M. Keck Foundation. The authors wish to recognize and acknowledge the very significant cultural role and reverence that the summit of Mauna Kea has always had within the indigenous Hawaiian community. We are most fortunate to have the opportunity to conduct observations from this mountain.

This work has made use of the NIST Atomic Spectra Database (ver. 3.1), available online at http://physics.nist.gov/asd3. C. T. acknowledges partial support from NASA through the American Astronomical Society's Small Research Grant Program and NASA grant NNG06GC36G. C. H. acknowledges support from NSF grant AST 04-06987. M. E. P. acknowledges support from the Research Corporation under a Cottrell Scholar Award.

[8] Note that Fig. 7 does not show the full extent of Complex C.

REFERENCES

Alibés, A., Labay, J., & Canal, R. 2001, A&A, 370, 1103
Belokurov, V., et al. 2006, ApJ, 647, L111
———. 2007, ApJ, 654, 897
Bregman, J. N. 1980, ApJ, 236, 577
Chiappini, C., Matteucci, F., & Romano, D. 2001, ApJ, 554, 1044
Collins, J. A., Shull, J. M., & Giroux, M. L. 2003, ApJ, 585, 336
———. 2007, ApJ, 657, 271
Danly, L., Albert, C. E., & Kuntz, K. D. 1993, ApJ, 416, L29
de Avillez, M. A. 2000, Ap&SS, 272, 23
de Heij, V., Braun, R., & Burton, W. B. 2002, A&A, 391, 159
Dorman, B. 1992, ApJS, 81, 221
Fenner, Y., & Gibson, B. K. 2003, Publ. Astron. Soc. Australia, 20, 189
Fox, A. J., Savage, B. D., Wakker, B. P., Richter, P., Sembach, K. R., & Tripp, T. M. 2004, ApJ, 602, 738
Gibson, B. K., Giroux, M. L., Penton, S. V., Stocke, J. T., Shull, J. M., & Tumlinson, J. 2001, AJ, 122, 3280
Girardi, L., Grebel, E. K., Odenkirchen, M., & Chiosi, C. 2004, A&A, 422, 205
Haffner, L. M., Reynolds, R. J., Tufte, S. L., Madsen, G. J., Jaehnig, K. P., & Percival, J. W. 2003, ApJS, 149, 405
Houck, J. C., & Bregman, J. N. 1990, ApJ, 352, 506

Hulsbosch, A. N. M., & Raimond, E. 1966, Bull. Astron. Inst. Netherlands, 18, 413
Kalberla, P. M. W., Burton, W. B., Hartmann, D., Arnal, E. M., Bajaja, E., Morras, R., & Pöppel, W. G. L. 2005, A&A, 440, 775
Kaufmann, T., Mayer, L., Wadsley, J., Stadel, J., & Moore, B. 2006, MNRAS, 370, 1612
Lee, Y.-S., et al. 2008, ApJ, submitted (arXiv:0710.5778)
Lockman, F. J. 2003, ApJ, 591, L33
Maller, A. H., & Bullock, J. S. 2004, MNRAS, 355, 694
Mateo, M. L. 1998, ARA&A, 36, 435
Mathewson, D. S., Cleary, M. N., & Murray, J. D. 1974, ApJ, 190, 291
Meggers, W. F., Corliss, C. F., Corliss, C. H., & Scribner, B. F. 1976, NBS Monogr. 145 (Washington: GPO), 1975
Muller, C. A., Oort, J. H., & Raimond, E. 1963, Comptes Rendus l'Acad. Sci., 257, 1661
Murphy, E. M., et al. 2000, ApJ, 538, L35
Oort, J. H. 1966, Bull. Astron. Inst. Netherlands, 18, 421
Oosterloo, T., Fraternali, F., & Sancisi, R. 2007, AJ, 134, 1019
Pagel, B. E. J., & Patchett, B. E. 1975, MNRAS, 172, 13
Peek, J. E. G., Putman, M. E., & Sommer-Larsen, J. 2008, ApJ, 674, 227
Putman, M. E., Staveley-Smith, L., Freeman, K. C., Gibson, B. K., & Barnes, D. G. 2003, ApJ, 586, 170
Putman, M. E., Thom, C., Gibson, B. K., & Staveley-Smith, L. 2004, ApJ, 603, L77
Richter, P., Sembach, K. R., Wakker, B. P., & Savage, B. D. 2001, ApJ, 562, L181
Ryan-Weber, E. V., et al. 2008, MNRAS, 384, 535
Ryans, R. S. I., Keenan, F. P., Sembach, K. R., & Davies, R. D. 1997, MNRAS, 289, 83
Savage, B. D., et al. 2000, ApJS, 129, 563
Schwarz, U. J., Wakker, B. P., & van Woerden, H. 1995, A&A, 302, 364
Sembach, K. R., & Savage, B. D. 1992, ApJS, 83, 147
Sembach, K. R., et al. 2003, ApJS, 146, 165
Siegel, M. H., Majewski, S. R., Gallart, C., Sohn, S. T., Kunkel, W. E., & Braun, R. 2005, ApJ, 623, 181
Simon, J. D., & Blitz, L. 2002, ApJ, 574, 726
Simon, J. D., Blitz, L., Cole, A. A., Weinberg, M. D., & Cohen, M. 2006, ApJ, 640, 270
Sirko, E., et al. 2004, AJ, 127, 899
Sommer-Larsen, J. 2006, ApJ, 644, L1
Thom, C. 2006, Ph.D. thesis, Swinburne Univ. Techn.
Thom, C., Putman, M. E., Gibson, B. K., Christlieb, N., Flynn, C., Beers, T. C., Wilhelm, R., & Lee, Y. S. 2006, ApJ, 638, L97
Tripp, T. M., et al. 2003, AJ, 125, 3122
Tufte, S. L., Reynolds, R. J., & Haffner, L. M. 1998, ApJ, 504, 773
van Woerden, H., Schwarz, U. J., Peletier, R. F., Wakker, B. P., & Kalberla, P. M. W. 1999, Nature, 400, 138
Vogt, S. S., et al. 1994, Proc. SPIE, 2198, 362
Wakker, B. P. 2001, ApJS, 136, 463
Wakker, B. P., Kalberla, P. M. W., van Woerden, H., de Boer, K. S., & Putman, M. E. 2001, ApJS, 136, 537
Wakker, B. P., Oosterloo, T. A., & Putman, M. E. 2002, AJ, 123, 1953
Wakker, B. P., & van Woerden, H. 1991, A&A, 250, 509
Wakker, B. P., van Woerden, H., Schwartz, U. J., Peletier, R. F., & Douglas, N. G. 1996, A&A, 306, L25
Wakker, B. P., York, D. G., Wilhelm, R., Barentine, J. C., Richter, P., Beers, T. C., Ivezić, Ž., & Howk, J. 2008, ApJ, 672, 298
Wakker, B. P., et al. 1999, Nature, 402, 388
———. 2007, ApJ, 670, L113
Westmeier, T., Braun, R., & Thilker, D. 2005, A&A, 436, 101
Wilhelm, R., Beers, T. C., & Gray, R. O. 1999, AJ, 117, 2308
Willman, B., Dalcanton, J., Ivezić, Ž., Schneider, D. P., & York, D. G. 2002, AJ, 124, 2600
Willman, B., et al. 2005a, AJ, 129, 2692
———. 2005b, ApJ, 626, L85